Comparison of the protective effects of chitosan oligosaccharides and chitin oligosaccharide on apoptosis, inflammation and oxidative stress

QIONGYU LI, WAN-RONG SHI and YUN-LIN HUANG

College of Chemical Engineering and Materials Science, Quanzhou Normal University, Quanzhou, Fujian 362000, P.R. China

Received November 6, 2023; Accepted April 26, 2024

DOI: 10.3892/etm.2024.12600

Abstract. Chitin degradation products, especially chitosan oligosaccharides (COSs), are highly valued in various industrial fields, such as food, medicine, cosmetics and agriculture, for their rich resources and high cost-effectiveness. However, little is known about the impact of acetylation on COS cellular bioactivity. The present study aimed to compare the differential effects of COS and highly N-acetylated COS (NACOS), known as chitin oligosaccharide, on H_2O_2-induced cell stress. MTT assay showed that pretreatment with NACOS and COS markedly inhibited H_2O_2-induced RAW264.7 cell death in a concentration-dependent manner. Flow cytometry indicated that NACOS and COS exerted an anti-apoptosis effect on H_2O_2-induced oxidative damage in RAW264.7 cells. NACOS and COS treatment ameliorated H_2O_2-induced RAW264.7 cell cycle arrest. Western blotting revealed that the anti-oxidation effects of NACOS and COS were mediated by suppressing expression of proteins involved in H_2O_2-induced apoptosis, including Bax, Bcl-2 and cleaved PARP. Furthermore, the antagonist effects of NACOS were greater than those of COS, suggesting that acetylation was essential for the protective effects of COS.

Introduction

Chitin, a cationic amino polysaccharide composed of N-acetylglucosamine linked by β-1,4-glycosidic bonds, is a natural macromolecule with a yield second only to cellulose in nature. It is commonly found in the shells of crustaceans, insect epidermis and fungal cell walls (1). Complete or partial deacetylation of chitin can yield chitosan, a cationic alkaline polysaccharide composed of D-glucosamine linked by β-1,4-glycosidic bonds. Degradation of chitosan produces chitosan oligosaccharides (COSs), characterized by low molecular weight and high biological activity (2). Moreover, chitin degradation results in the production of N-acetylated COS (NACOS), which exhibits good solubility and multiple biological functions, including antioxidant, anti-inflammatory, antitumor, antimicrobial and plant elicitor activities, as well as immunomodulatory and prebiotic effects (3). While chitin and its derivative chitosan are known for their various functional activities, their limited solubility hinders their use in food and biomedical applications. However, hydrolyzed products of chitosan, including COS (3-5) and NACOS, exhibit increased water solubility due to their shorter chain length, lower viscosity and potentially higher absorption rates (6-8).

Numerous studies have shown that COS and its derivatives possess biological activities, including anti-inflammation, anti-tumor, anti-obesity, anti-Alzheimer's disease, immunostimulation, tissue regeneration promotion, drug and DNA delivery enhancement, anti-microbiome and anti-oxidation effects (5,9-12). Some studies also report that COS possesses robust neuroprotective properties, such as β-amyloid and acetylcholinesterase inhibition, anti-neuroinflammation and anti-apoptosis (13,14). COS has demonstrated its potential to mitigate high-fat diet-induced obesity and insulin resistance by modulating gut microbiota dysfunction, mitigating low-grade inflammation and preserving the integrity of the intestinal epithelial barrier (15). Inflammatory factors serve an important role in cardiovascular diseases such as atherosclerosis, myocardial infarction and cardiac failure (16). Several studies have highlighted the anti-inflammatory effects of COS (17,18). The mechanism underlying the anti-inflammatory effects of orally administered COS may involve suppressing inflammatory processes, including regulating the expression of NF-κB, Nrf2, TGF-β1/Smad, inducible nitric oxide synthase and pro-inflammatory cytokines (15). Notably, COS has been shown to extend the survival of mice challenged with lipopolysaccharide (19).

Oxidative stress and inflammation are linked, with their interdependence consistently documented. Emerging evidence implicates oxidative stress in various types of diseases, including diabetes (20), atherosclerosis (21) and cancer (22), as well as aging (23), prompting attention to the role of antioxidants in biological systems. Extensive efforts have been devoted to identifying suitable antioxidant compounds for preventive and therapeutic purposes. Reactive oxygen species (ROS), such as superoxide anion (O_2^-), H_2O_2

Correspondence to: Dr Qiongyu Li, College of Chemical Engineering and Materials Science, Quanzhou Normal University, 398 Donghai Street, Fengze, Quanzhou, Fujian 362000, P.R. China
E-mail: 1348097881@qq.com

Key words: N-acetylated chitosan oligosaccharide, apoptosis

and hydroxyl radicals (HO^-), are continually generated at a substantial rate as by-products of aerobic metabolism and radiation exposure (24). These oxidants not only damage cellular macromolecules, including DNA, protein and lipids, but also contribute to NLRP3 inflammasome activation and mediate inflammatory responses, establishing a cycle of localized inflammation leading to oxidative damage (25). The persistent threat of oxidant-induced damage to cells, tissue and organisms is underscored by cellular defense mechanisms evolved to combat reactive oxidants. Excessive ROS is readily converted to H_2O_2, which easily diffuses across cell membranes and generates highly reactive and toxic hydroxyl radicals via the heme-catalyzed Fenton reaction, leading to rapid DNA damage and strand breaks when superoxide anions react with nitric oxide (NO) to form peroxynitrite, a reactive nitrogen species (23). In response to oxidative stress-induced DNA damage, processes such as cell cycle arrest and DNA damage repair are initiated as cellular defense mechanisms. However, if DNA damage exceeds the cell repair capacity, it ultimately leads to apoptotic cell death (26). Macrophages are key immune cells for the host defense system to eliminate microbial pathogens. Studies have verified that macrophages can produce ROS when infected by some bacteria, making them a suitable model for antioxidant research (27,28). The mouse macrophage cell line RAW264.7 is the most commonly used mouse macrophage cell line in medical research (29). Therefore, the present study used H_2O_2-stimulated RAW264.7 cells to establish a cellular oxidative damage model.

COS has shown potential in protecting against oxidative stress-induced cell damage by modulating enzyme activity and gene expression related to antioxidant defense mechanisms (25,30-33), thus exerting health benefits primarily through antioxidant activity. Scholars have highlighted the impact of physicochemical parameters such as molecular weight and degree of acetylation (DA) on the bioactivities of COS (34,35). However, the lack of well-defined and standardized criterion for distinguishing the bioactivity of COS with varying degrees of polymerization is compounded by the shared nomenclature of COS and NACOS, leading to potential confusion. Therefore, the present study aimed to investigate the impact of acetylation on COS biological activity by comparing the protective effects of deacetylated COS and its non-deacetylated form, NACOS, on H_2O_2-induced apoptosis and oxidative stress in RAW264.7 cells.

Materials and methods

Chemicals and reagents. Dulbecco's modified Eagle's medium (DMEM) medium was purchased from Corning, Inc. Fetal bovine serum (FBS), penicillin and streptomycin were from Gibco (Thermo Fisher Scientific, Inc.). Annexin V-FITC kit and Cell Cycle Analysis kit were from Beyotime Institute of Biotechnology. Colored standards and all the other reagents for SDS-PAGE and immunoblotting were from Bio-Rad Laboratories, Inc. Antibodies against β-actin, Bax, Bcl-2, PARP and cleaved PARP, as well as horseradish peroxidase (HRP)-conjugated goat anti-rabbit IgG and HRP-conjugated goat anti-mouse IgG were obtained from Cell Signaling Technology, Inc. All chemicals used were analytical grade unless otherwise stated.

Purification and quantitative analysis of NACOS and COS. COS with a deacetylation degree of 88% and polymerization degree of 2-6 was prepared through enzymatic hydrolysis of chitosan, as described previously (36). NACOS was also prepared as described previously (37). In brief, COS was dissolved in 50 ml water with 3 ml methanol, 0.1 g 4-dimethylaminopyridine and 4.37 ml acetic anhydride. The mixture was incubated at 60˚C for 4 h. Subsequently, 5X the volume of acetone was added to obtain NACOS. DA and polymerization degree were determined using liquid chromatography-mass spectrometry and nuclear magnetic resonance analyses by Institute of Process Engineering, Chinese Academy of Sciences. The mass spectrometry detection conditions were: ESI source; positive ion scanning mode; 3 kV capillary voltage; 60 V cone hole voltage; 150˚C ion source temperature; 500˚C desolvent gas temperature; 50 l/h flow rate of conical hole gas; 800 l/h desolvent gas flow rate; 150-2,000 m/z quality scanning range.

Cell culture. The mouse monocyte macrophage leukemia RAW264.7 cell line was obtained from the Type Culture Collection of the Chinese Academy of Sciences. RAW264.7 cells were cultured in DMEM supplemented with 5% heat-inactivated FBS, 100 U/ml penicillin and 100 μg/ml streptomycin in a humidified atmosphere with 5% CO_2 at 37˚C and passaged twice/week. Cells at a confluence of 70-80% were used for subsequent experiments.

Identification of cell viability using MTT assay. Cell viability was determined by MTT colorimetric assay. In brief, cells were treated with NACOS and COS (25, 50 or 100 μg/ml) for 12 h at 37˚C and cell viability was detected by MTT assay. In addition, cells were pretreated with NACOS and COS (25, 50 or 100 μg/ml) for 12 h at 37˚C, followed by 300 μM H_2O_2 for another 12 h at 37˚C. Treatment with equal volume PBS was included as the vehicle control. A total of 100 μl 0.5 mg/ml MTT PBS solution was added to each well and the samples were incubated for an additional 4 h at 37˚C. The purple-blue MTT formazan precipitate was dissolved in 100 μl dimethyl sulfoxide and the absorbance at 570 nm was measured using a microplate reader.

Identification of cell cycle stage by propidium iodide (PI) staining. Cell cycle analysis was performed by flow cytometry using a fluorescence-activated cell sorting (FACS) MoFlo XDP (Beckman Coulter) following PI staining. In brief, RAW264.7 cells were exposed to 50 μg/ml NACOS and COS for 12 h and stimulated with 300 μM H_2O_2 for another 12 h at 37˚C. The cells were harvested, adjusted to a concentration of $1x10^6$ cells/ml by cell count and dilution, and fixed in 70% ethanol at 4˚C overnight. The fixed cells were washed twice with cold PBS and incubated with RNase (8 μg/ml) and PI (10 μg/ml) at 4˚C for 30 min. The fluorescent signal was detected through the FL2 channel and the proportion of DNA in various phases was analyzed using ModfitLT Version 3.0 (Verity Software House, Inc.).

Identification of apoptosis by Annexin V/PI staining. A total of $2x10^5$ RAW264.7 cells in 2 ml DMEM complete medium

was seeded into 6-well plates and treated with 50 μg/ml NACOS or COS for 12 h and then stimulated with 300 μM H_2O_2 for another 12 h at 37˚C. Apoptosis of RAW264.7 cells was determined by flow cytometry analysis using a FACS caliber (Becton-Dickinson) and Annexin V-fluorescein isothiocyanate (FITC)/PI kit. Cell apoptosis was quantified using FlowJo software (v.10.1.1; FlowJo LLC). Staining was performed according to the manufacturer's instructions. Annexin V/PI double-negative population represented viable cells, while Annexin V-positive/PI-negative or Annexin V/PI double-positive population represented cells undergoing early or late apoptosis, respectively.

Reverse transcription-quantitative polymerase chain reaction (RT-qPCR) analysis. The total RNA was isolated from cells using RNAisoPlus reagent (Takara Biotechnology Co., Ltd.). Reverse transcription into cDNA was amplified according to the manufacturer's instructions using the PrimeScript RT reagent kit (Takara Biotechnology Co., Ltd.). An ABI 7500 Fast Real-Time PCR System (Applied Biosystems) and the SYBR Premix Ex Tag (Takara Biotechnology Co., Ltd.) was used for PCR. Following an initial denaturation at 95˚C for 5 min, the PCR conditions were as follows: 35 cycles of denaturation at 95˚C for 30 sec, annealing at 55˚C for 30 sec and extension at 72˚C for 30 sec. The $2^{-\Delta\Delta Cq}$ method was used to calculate the mRNA expression levels in each sample (38). Data were normalized to the GAPDH content of the sample. The primer sequences were as follows: L-1β forward, 5'-ATGATGGCT TATTACAGTGGCAA-3' and reverse 5'-GTCGGAGATTCG TAGCTGGA-3'; IL-6 forward, 5'-ACTCACCTCTTCAGA ACGAATTG-3' and reverse, 5'-CCATCTTTGGAAGGT TCAGGTTG-3'; IL-8 forward, 5'-ACTGAGAGTGATTGA GAGTGGAC-3' and reverse, 5'-AACCCTCTGCACCCAGTT TTC-3'; TNF-α forward, 5'-CCTCTCTCTAATCAGCCCTCT G-3' and reverse, 5'-GAGGACCTGGGAGTAGATGAG-3'; MCP-1 forward, 5'-CAGCCAGATGCAATCAATGCC-3' and reverse, 5'-TGGAATCCTGAACCCACTTCT-3'; and GAPDH forward, 5'-CACATGGCCTCCAAGGAGTAA-3' and reverse, 5'-TGAGGGTCTCTCTCTTCCTCTTGT-3'.

Western blot analysis. Total protein extracts were obtained using RIPA lysis buffer and concentrations were determined by the BCA assay (both Pierce; Thermo Fisher Scientific, Inc.). Equal amounts of protein (50 μg) from each sample were separated using 10-15% SDS-PAGE and transferred onto PVDF membranes. The membranes were blocked with 5% non-fat milk for 1 h at room temperature and incubated with specific primary antibodies (all 1:1,000) against Bcl-2 (cat. no. 4223), Bax (cat. no. 5023), PARP, cleaved-PARP (cat. no. 9542) and β-actin (cat. no. 4697) from Cell Signaling Technology, Inc., at 4˚C overnight. After incubating with horseradish peroxidase-conjugated secondary antibodies (1:250,000) at room temperature for 2 h, the signals were visualized using enhanced chemiluminescence. Protein bands were visualized using enhanced chemiluminescence reagent (Thermo Fisher Scientific, Inc.). Protein expression levels were semi-quantified using ImageJ software (v2.1.4.7) with β-actin as the loading control.

Statistical analysis. All experiments were performed three times independently. All data are presented as the mean ± SD.

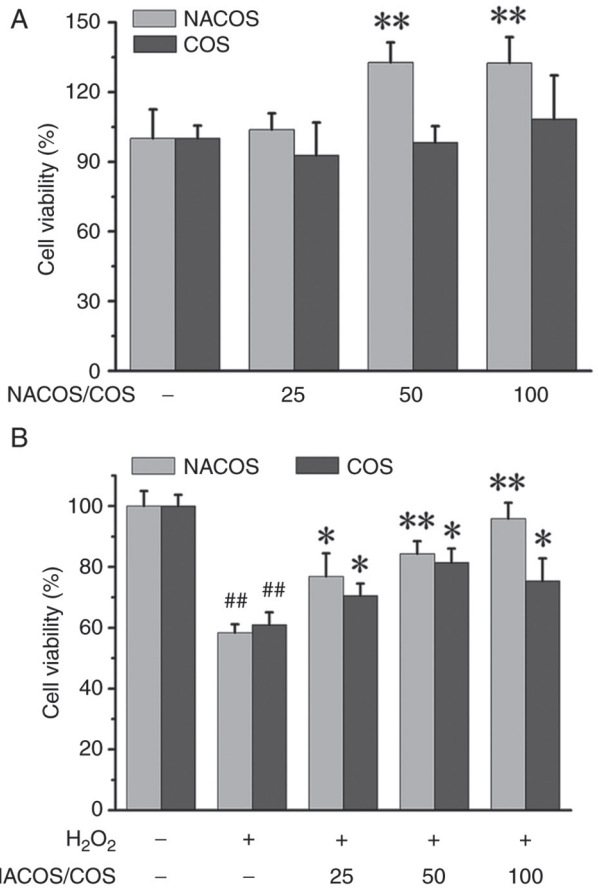

Figure 1. Effects of NACOS and COS on viability of RAW264.7 macrophage cells. (A) Cells were treated with NACOS (25-100 μg/ml) or COS (25-100 μg/ml) for 12 h and cell viabilities were determined by MTT assay. (B) Effects of NACOS and COS on H_2O_2-treated macrophage cells. Cells were pre-treated with NACOS (25-100 μg/ml) or COS (25-100 μg/ml) for 15 h and then exposed to H_2O_2 (300 μM) for 12 h. After that, cells were collected for viability detection by MTT assay. n=3. $^{##}$P<0.01 vs. control; *P<0.05, **P<0.01 vs. H_2O_2-alone.

Data were analyzed by one-way ANOVA followed by Tukey-Kramer's post hoc test. P<0.05 was considered to indicate a statistically significant difference. All statistical analysis was performed using the SPSS package for Windows (version 17.0; SPSS, Inc.).

Results

Effects of NACOS and COS on viability of H_2O_2-stimulated RAW264.7 cells. MTT assay was performed to assess the potential cytotoxic effects of NACOS and COS treatments. The results of liquid chromatography-mass spectrometry and nuclear magnetic resonance analyses indicated that obtained COS had a deacetylation degree of 88% and polymerization degree of 2-6, while NACOS had a deacetylation degree of 97% and a polymerization degree of 3-10 (Fig. S1). COS (25, 50 or 100 μg/ml) for 24 h did not lead to a reduction in RAW264.7 cell viability. By contrast, NACOS at 50 and 100 μg/ml remarkably increased cell viability (Fig. 1A). Subsequently, the effects of NACOS and COS on the viability of RAW264.7 cells was assessed following H_2O_2-treatment. H_2O_2 led to a substantial decrease in cell

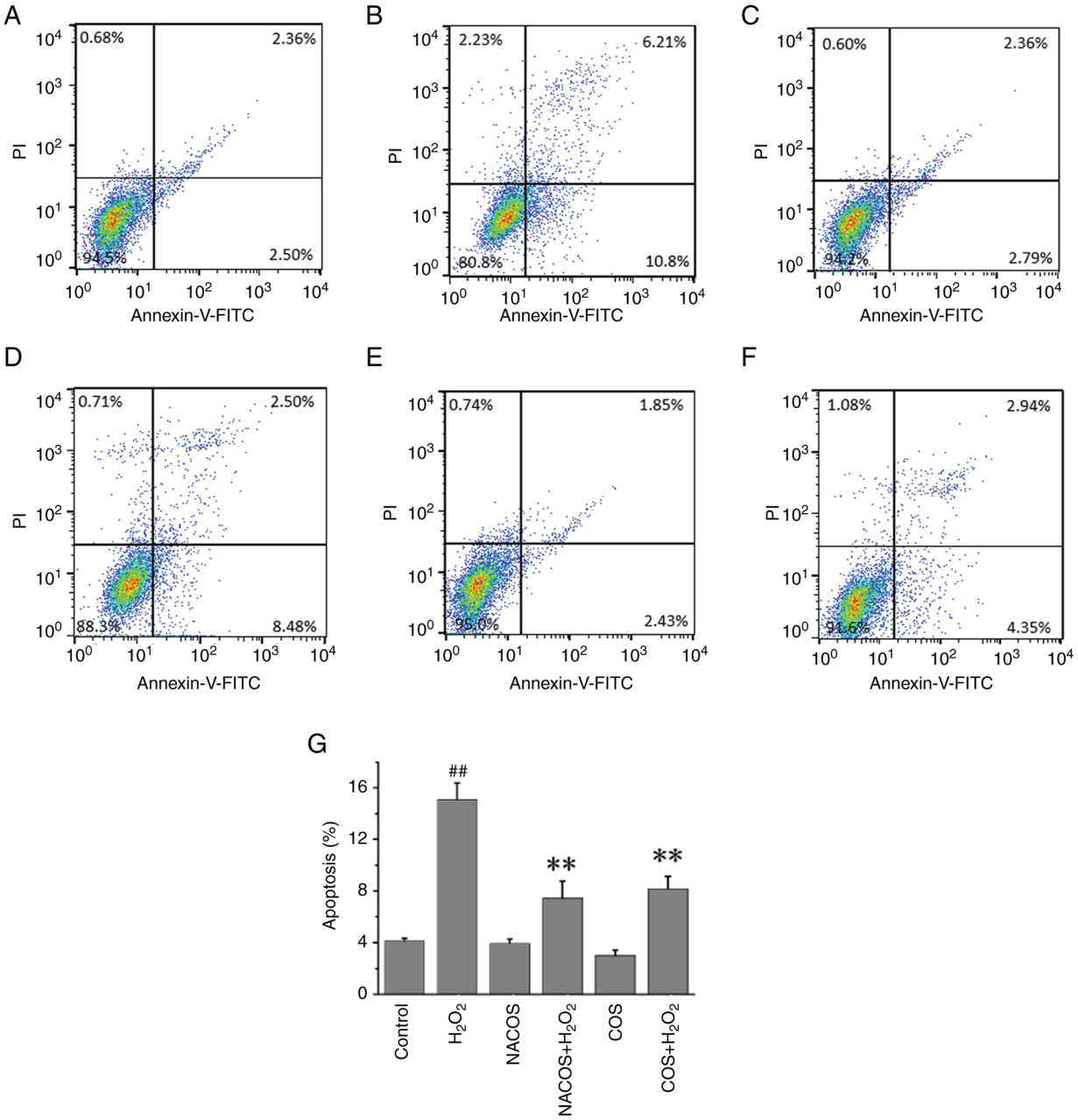

Figure 2. Effects of NACOS and COS on H_2O_2-induced apoptosis in RAW264.7 macrophage cells. Cells were pre-treated with NACOS or COS (both 100 μg/ml) for 12 h, then exposed to H_2O_2 (300 μM) for 12 h. Then, cells were labeled with a combination of PI and Annexin V-FITC for flow cytometric analysis. Representative flow cytometric histograms of (A) control, (B) H_2O_2-alone (C) NACOS, (D) NACOS + H_2O_2, (E) COS and (F) COS + H_2O_2 group. (G) Apoptotic rate. n=3. $^{##}$P<0.01 vs. control; **P<0.01 vs. H_2O_2-alone.

viability, reaching 37.60±0.56% compared with untreated controls. However, NACOS and COS treatment effectively attenuated the inhibitory effects of H_2O_2 on cell viability. However, 100 μg/ml COS had less effect than 50 μg/ml COS (Fig. 1B). NACOS and COS at 100 μg/ml resulted in a significant increase compared with H_2O_2 alone in terms of cell viability, with values of 8.61±0.34 and 6.27±0.63%, respectively. This protective effect of NACOS/COS may be associated with scavenging of oxygen free radicals. Both NACOS and COS effectively scavenged oxygen free radicals, albeit with varying scavenging abilities and impacts on different types of oxygen free radicals, including ·OH, $\cdot O_2^-$, NO· and DPPH· (Table SI).

NACOS and COS protect against H_2O_2-induced cellular apoptosis. Flow cytometry showed that 15.74% of cells underwent apoptosis following treatment with H_2O_2 alone, which was significantly higher than that of untreated control cells. However, only 6.94 and 8.16% of cells that were pretreated with COS or NACOS, respectively, (100 μg/ml) for 24 h underwent apoptosis following H_2O_2 treatment, showing a significant difference compared with H_2O_2 alone (Fig. 2). NACOS and COS pretreatment protected against cellular apoptosis induced by oxidative stress. In addition, NACOS and COS decreased mRNA expression of IL-1β, IL-6, TNF-α and MCP-1 in H_2O_2-stimulated RAW264.7 cells (Fig. S2).

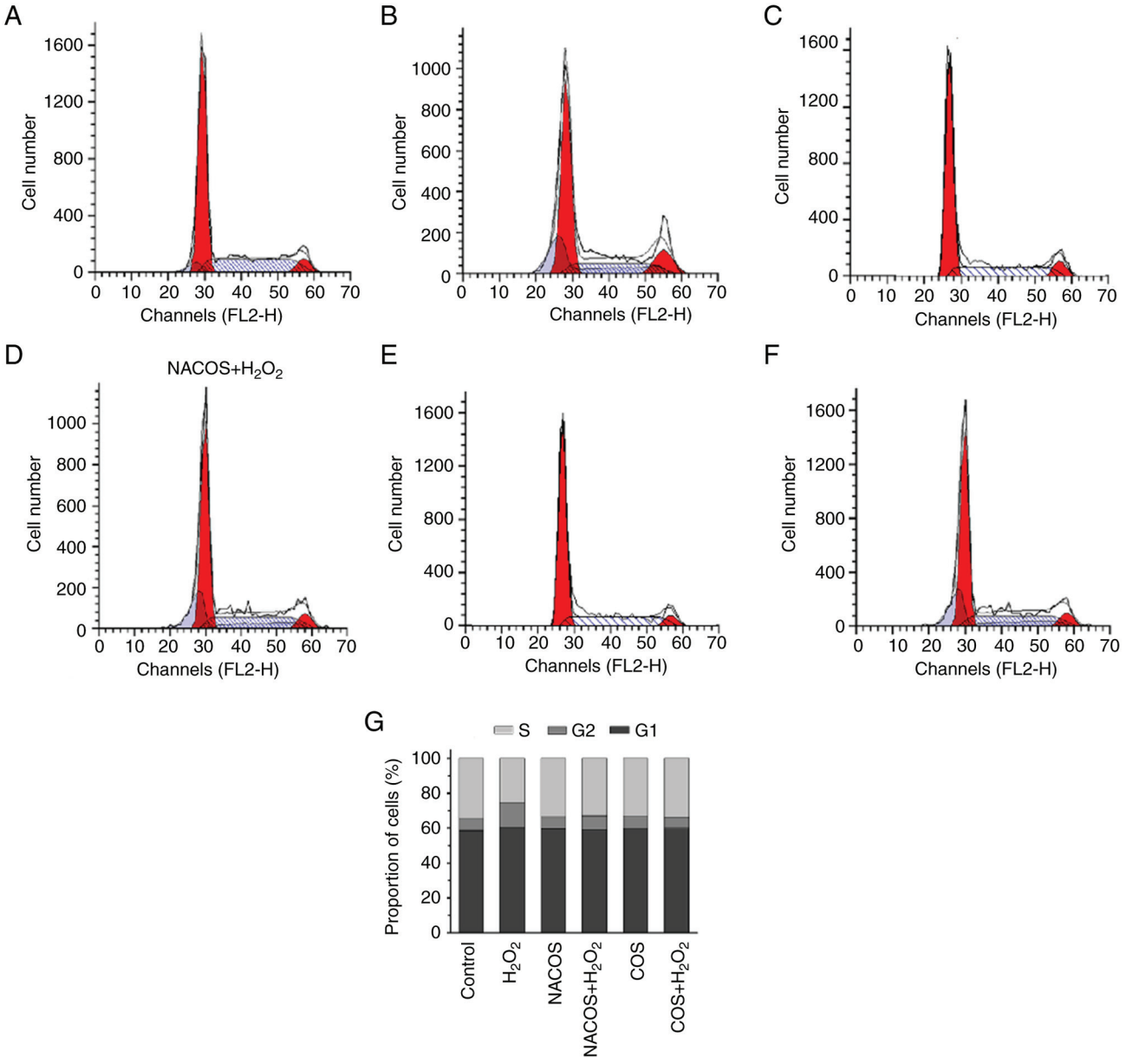

Figure 3. Effect of NACOS and COS on H_2O_2-induced cell cycle arrest. (A) RAW264.7 cells were pre-treated with NACOS or COS (both 100 μg/ml) for 12 h and exposed to H_2O_2 (300 μM) for 12 h. Cells were collected and incubated with PI for flow cytometric analysis. Representative flow cytometric histograms of (A) control, (B) H_2O_2-alone (C) NACOS, (D) NACOS + H_2O_2, (E) COS and (F) COS + H_2O_2. (G) Cell cycle distribution.

Cell cycle changes following NACOS and COS treatment. Effects of NACOS and COS treatment on H_2O_2-induced G1/S phase arrest of RAW264.7 cells was assessed using FACS analysis. The results showed that COS or NACOS alone had no significant effect on the proportion of cells at different phases. The percentage of S phase cells was increased by up to 10% following treatment with 100 μg/ml NACOS and COS compared with H_2O_2 alone (Fig. 3), indicating that NACOS and COS prevented H_2O_2-induced G1/S cell cycle arrest.

Effect of NACOS and COS on PARP cleavage and Bcl-2 expression. PARP, a 116 kDa nuclear poly(ADP-ribose) polymerase involved in DNA repair and cell proliferation, is be cleaved by caspase-3, serving as an indicator of apoptotic cells (39). H_2O_2 is widely recognized for inducing PARP cleavage (40). H_2O_2 treatment increased the levels of cleaved PARP compared with untreated control, confirming that H_2O_2 triggered cellular apoptosis (Fig. 4). However, pretreatment with COS and NACOS significantly inhibited PARP cleavage, suggesting both COS and NACOS prevented H_2O_2-induced apoptosis in RAW264.7 cells. Moreover, the effect of NACOS in protecting against cellular apoptosis was superior to that of COS. The rescue of cellular apoptosis is typically associated with the upregulation of anti-apoptotic molecules such as Bcl-2, which function in antioxidant pathways to prevent apoptosis (41). Bax is also an apoptotic-induced protein (42). COS and NACOS upregulated Bcl-2 and downregulated Bax protein expression following H_2O_2 treatment (Fig. 4). Moreover, NACOS showed a superior protective effect compared with COS.

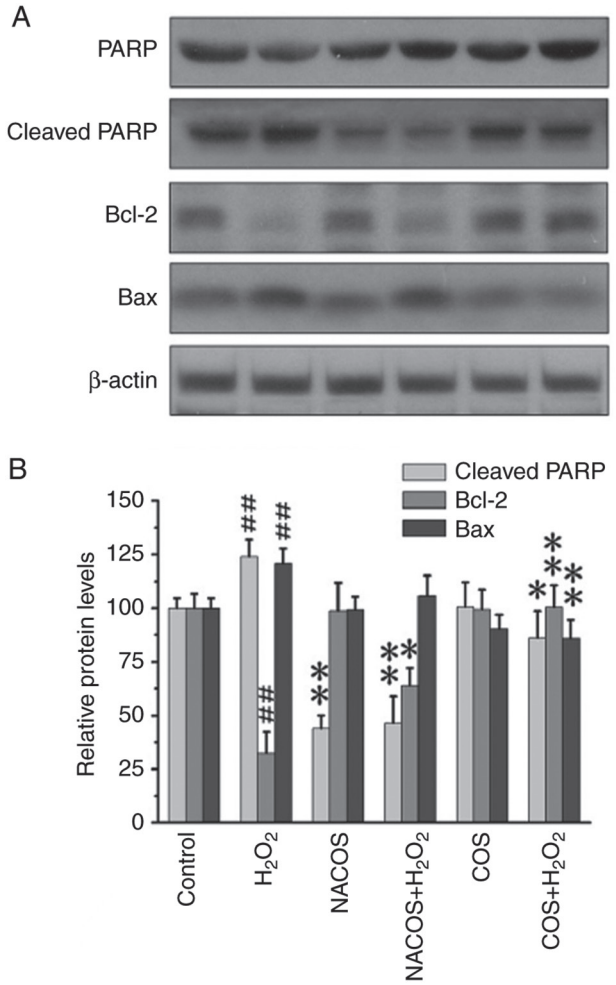

Figure 4. Effect of NACOS and COS on apoptotic protein expression. (A) Cells were pre-treated with NACOS or COS (both 100 μg/ml) for 12 h and then exposed to H_2O_2 (300 μM) for 12 h. The expression of Bax, Bcl-2, PARP and cleaved PARP following NACOS and COS treatment in RAW264.7 cells was determined by western blot analysis. (B) Densitometric analysis was performed to determine protein expression fold change. The protein expression of cleaved PARP was normalized to that of PARP. $^{\#\#}$P<0.01 vs. control; *P<0.05, **P<0.01 vs. H_2O_2-alone.

Discussion

The present study compared the antioxidant activities of NACOS and COS against H_2O_2-induced oxidative damage. NACOS and COS effectively attenuated oxidative stress induced by H_2O_2. Although COS did not significantly affect cell viability, NACOS treatment significantly increased cell viability. The improvement of cell viability by NACOS may be associated to its antioxidant, antiapoptotic, cell proliferation induction or cell cycle regulation effects, suggesting the need for further investigation into the underlying mechanism. Furthermore, both NACOS and COS significantly attenuated H_2O_2-induced inhibition of cell viability in a concentration-dependent manner. Cell cycle assay revealed that NACOS and COS reversed H_2O_2-induced inhibition of G1/S cell cycle arrest and significantly mitigated H_2O_2-induced cell apoptosis. The protective effects of NACOS and COS may be attributed to their ability to scavenge oxygen free radicals, thereby preventing oxidative damage.

Previous studies have suggested that COS exerts potential free radical scavenging properties through both direct and indirect mechanisms (43,44). Here, both NACOS and COS effectively scavenged oxygen free radicals, albeit with varying scavenging abilities and impacts on different types of oxygen free radicals. Thus, both COS and NACOS inhibited molecular damage by scavenging free radicals in cells.

Furthermore, both NACOS and COS protected against H_2O_2-induced apoptosis, as observed by flow cytometry. Previous studies have also indicated that COS enhances cell viability following H_2O_2 treatment and decreases apoptosis rate (45,46). In addition, COS increases extracellular matrix synthesis and prevents its degradation (47). Here, highly acetylated NACOS notably inhibited H_2O_2-induced apoptosis. Furthermore, the protective effect of NACOS was greater than that of COS. Previous studies have indicated that degree of polymerization plays a critical role in the neuroprotective effects of COS (47). β-amyloid (Aβ) aggregates containing cross-β-sheet structures induce oxidative stress, neuroinflammation and neuronal loss via multiple pathways. COS can directly bind to Aβ42 in a polymerization-dependent manner, ameliorating Aβ42-induced cytotoxicity (48).

Mitochondria serve as central integrators and transducers of various pro-apoptotic signals, with their disruption and subsequent release of pro-apoptotic proteins being a key aspect of the apoptosis process (49,50). The release of these factors from mitochondria is regulated by Bcl-2 family proteins, which are key regulators for cell apoptosis under both normal and oxidative stress conditions (41,51). The present study showed that both NACOS and COS increased Bcl-2 expression and protected against H_2O_2-induced apoptosis in RAW264.7 cells. Furthermore, activation of effector caspases, such as caspase-3, leads to PARP cleavage, resulting in apoptosis (52). Here, cleaved PARP expression was ameliorated following NACOS and COS treatments in RAW264.7 cells, with the effects of NACOS superior to those of COS. These findings suggested that acetylation may be essential for the protective effects of COS.

The present findings suggest that the anti-apoptotic effect of COS and NACOS was associated with DA. Both COS and NACOS were effective in inhibiting oxidative damage induced by H_2O_2, with the antagonistic effect of NACOS greater than that of COS. This implied that the degree of deacetylation was positively associated with the protective effects of COS. Acetylation has been reported to facilitate passive diffusion of disaccharides across cell membranes, enabling them to enter the Golgi (53). Thus, acetylation modification may facilitate the entry of NACOS into cells, allowing them to interfere with ROS-induced apoptosis; however, the specific underlying mechanism requires further investigation. DA may be a key factor influencing the ability of COS to prevent oxidative damage-induced cell apoptosis. However, functional gain or loss analysis experiments are needed. NACOS and COS decreased mRNA expression of IL-1β, IL-6, TNF-α and MCP-1 in H_2O_2 stimulated RAW264.7 cells and the potential anti-inflammatory mechanisms of NACOS and COS may associated with promoting protein O-GlcNA acylation, which significantly inhibits the phosphorylation and nuclear translocation of inflammatory transcription factors (54). However, the specific underlying mechanism requires further investigation.

Acknowledgements

Not applicable.

Funding

The present study was supported by the Natural Science Foundation of Fujian Province of China (grant no. 2021J05057).

Availability of data and materials

The data generated in the present study may be requested from the corresponding author.

Authors' contributions

QL designed the study, analyzed data and wrote the manuscript. QL, WS and YH performed the experiments. QL and WS confirm the authenticity of all the raw data. All authors have read and approved the final manuscript.

Ethics approval and consent to participate

Not applicable.

Patient consent for publication

Not applicable.

Competing interests

The authors declare that they have no competing interests.

References

1. Satitsri S and Muanprasat C: Chitin and chitosan derivatives as biomaterial resources for biological and biomedical applications. Molecules 25: 5961, 2020.
2. Guan G, Azad MAK, Lin Y, Kim SW, Tian Y, Liu G and Wang H: Biological effects and applications of chitosan and chito-oligosaccharides. Front Physiol 10: 516, 2019.
3. Shahbaz U: Chitin, characteristic, sources, and biomedical application. Curr Pharm Biotechnol 21: 1433-1443, 2020.
4. Wang W, Meng Q, Li Q, Liu J, Zhou M, Jin Z and Zhao K: Chitosan derivatives and their application in biomedicine. Int J Mol Sci 21: 487, 2020.
5. Naveed M, Phil L, Sohail M, Hasnat M, Baig MMFA, Ihsan AU, Shumzaid M, Kakar MU, Mehmood Khan T, Akabar MD, *et al*: Chitosan oligosaccharide (COS): An overview. Int J Biol Macromol 129: 827-843, 2019.
6. Fan Z, Wang L, Qin Y and Li P: Activity of chitin/chitosan/chitosan oligosaccharide against plant pathogenic nematodes and potential modes of application in agriculture: A review. Carbohydr Polym 306: 120592, 2023.
7. Zheng J, Cheng G, Li Q, Jiao S, Feng C, Zhao X, Yin H, Du Y and Liu H: Chitin oligosaccharide modulates gut microbiota and attenuates high-fat-diet-induced metabolic syndrome in mice. Mar Drugs 16: 66, 2018.
8. Yuan X, Zheng J, Jiao S, Cheng G, Feng C, Du Y and Liu H: A review on the preparation of chitosan oligosaccharides and application to human health, animal husbandry and agricultural production. Carbohydr Polym 220: 60-70, 2019.
9. Lan R, Chang Q, Wei L and Zhao Z: The protect effects of chitosan oligosaccharides on intestinal integrity by regulating oxidative status and inflammation under oxidative stress. Mar Drugs 19: 57, 2021.
10. Hao C, Wang W, Wang S, Zhang L and Guo Y: An overview of the protective effects of chitosan and acetylated chitosan oligosaccharides against neuronal disorders. Mar Drugs 15: 89, 2017.
11. Zhai X, Yuan S, Yang X, Zou P, Shao Y, Abd El-Aty AM, Hacımüftüoğlu A and Wang J: Growth-inhibition of S180 residual-tumor by combination of cyclophosphamide and chitosan oligosaccharides in vivo. Life Sci 202: 21-27, 2018.
12. Shagdarova B, Konovalova M, Varlamov V and Svirshchevskaya E: Anti-obesity effects of chitosan and its derivatives. Polymers (Basel) 15: 3967, 2023.
13. Hao C, Han M, Wang W, Yang C, Wang J, Guo Y, Xu T, Zhang L and Li C: The neuroprotective effects of peracetylated chitosan oligosaccharides against β-amyloid-induced cognitive deficits in rats. Mar Life Sci Technol 5: 211-222, 2023.
14. Wang B, Wang L, Qu Y, Lu J and Xia W: Chitosan oligosaccharides exert neuroprotective effects via modulating the PI3K/Akt/Bcl-2 pathway in a Parkinsonian model. Food Funct 13: 5838-5853, 2022.
15. He N, Wang S, Lv Z, Zhao W and Li S: Low molecular weight chitosan oligosaccharides (LMW-COSs) prevent obesity-related metabolic abnormalities in association with the modification of gut microbiota in high-fat diet (HFD)-fed mice. Food Funct 11: 9947-9959, 2020.
16. Patoulias D, Stavropoulos K, Imprialos K, Athyros V, Grassos H, Doumas M and Faselis C: Inflammatory markers in cardiovascular disease; lessons learned and future perspectives. Curr Vasc Pharmacol 19: 323-342, 2021.
17. Yu Y, Luo T, Liu S, Song G, Han J, Wang Y, Yao S, Feng L and Qin S: Chitosan oligosaccharides attenuate atherosclerosis and decrease non-HDL in ApoE-/- mice. J Atheroscler Thromb 22: 926-941, 2015.
18. Yu Y, Wang S, Chen X, Gao Z, Dai K, Wang J and Liu C: Sulfated oligosaccharide activates endothelial Notch for inducing macrophage-associated arteriogenesis to treat ischemic diseases. Proc Natl Acad Sci USA 120: e2307480120, 2023.
19. Guo C, Zhang Y, Ling T, Zhao C, Li Y, Geng M, Gai S, Qi W, Luo X, Chen L, *et al*: Chitosan oligosaccharides alleviate colitis by regulating intestinal microbiota and PPARγ/SIRT1-Mediated NF-κB pathway. Mar Drugs 20: 96, 2022.
20. Zhang P, Li T, Wu X, Nice EC, Huang C and Zhang Y: Oxidative stress and diabetes: Antioxidative strategies. Front Med 14: 583-600, 2020.
21. Batty M, Bennett MR and Yu E: The role of oxidative stress in atherosclerosis. Cells 11: 3843, 2022.
22. Hayes JD, Dinkova-Kostova AT and Tew KD: Oxidative stress in cancer. Cancer Cell 38: 167-197, 2020.
23. Jomova K, Raptova R, Alomar SY, Alwasel SH, Nepovimova E, Kuca K and Valko M: Reactive oxygen species, toxicity, oxidative stress, and antioxidants: Chronic diseases and aging. Arch Toxicol 97: 2499-2574, 2023.
24. Sies H, Berndt C and Jones DP: Oxidative stress. Annu Rev Biochem 86: 715-748, 2017.
25. Steven S, Frenis K, Oelze M, Kalinovic S, Kuntic M, Bayo Jimenez MT, Vujacic-Mirski K, Helmstädter J, Kröller-Schön S, Münzel T and Daiber A: Vascular inflammation and oxidative stress: Major triggers for cardiovascular disease. Oxid Med Cell Longev 2019: 7092151, 2019.
26. Senoner T and Dichtl W: Oxidative stress in cardiovascular diseases: Still a therapeutic target? Nutrients 11: 2090, 2019.
27. Zhu H, Jia Z, Zhang L, Yamamoto M, Misra HP, Trush MA and Li Y: Antioxidants and phase 2 enzymes in macrophages: Regulation by Nrf2 signaling and protection against oxidative and electrophilic stress. Exp Biol Med (Maywood) 233: 463-474, 2008.
28. Grom AA and Mellins ED: Macrophage activation syndrome: Advances towards understanding pathogenesis. Curr Opin Rheumatol 22: 561-566, 2010.
29. Li P, Hao Z, Wu J, Ma C, Xu Y, Li J, Lan R, Zhu B, Ren P, Fan D and Sun S: Comparative proteomic analysis of polarized human THP-1 and mouse RAW264.7 macrophages. Front Immunol 12: 700009, 2021.
30. Mei QX, Hu JH, Huang ZH, Fan JJ, Huang CL, Lu YY, Wang XP and Zeng Y: Pretreatment with chitosan oligosaccharides attenuate experimental severe acute pancreatitis via inhibiting oxidative stress and modulating intestinal homeostasis. Acta Pharmacol Sin 42: 942-953, 2021.
31. Yang Z, Hong W, Zheng K, Feng J, Hu C, Tan J, Zhong Z and Zheng Y: Chitosan oligosaccharides alleviate H_2O_2-stimulated granulosa cell damage via HIF-1α signaling pathway. Oxid Med Cell Longev 2022: 4247042, 2022.
32. Wu J, Xu Y, Geng Z, Zhou J, Xiong Q, Xu Z, Li H and Han Y: Chitosan oligosaccharide alleviates renal fibrosis through reducing oxidative stress damage and regulating TGF-β1/Smads pathway. Sci Rep 12: 19160, 2022.

33. Wang Y, Xiong Y, Zhang A, Zhao N, Zhang J, Zhao D, Yu Z, Xu N, Yin Y, Luan X and Xiong Y: Oligosaccharide attenuates aging-related liver dysfunction by activating Nrf2 antioxidant signaling. Food Sci Nutr 8: 3872-3881, 2020.
34. Hao W, Li K, Ge X, Yang H, Xu C, Liu S, Yu H, Li P and Xing R: The effect of N-acetylation on the anti-inflammatory activity of chitooligosaccharides and its potential for relieving endotoxemia. Int J Mol Sci 23: 8205, 2022.
35. Abd El-Hack ME, El-Saadony MT, Shafi ME, Zabermawi NM, Arif M, Batiha GE, Khafaga AF, Abd El-Hakim YM and Al-Sagheer AA: Antimicrobial and antioxidant properties of chitosan and its derivatives and their applications: A review. Int J Biol Macromol 164: 2726-2744, 2020.
36. Zheng J, Yuan X, Cheng G, Jiao S, Feng C, Zhao X, Yin H, Du Y and Liu H: Chitosan oligosaccharides improve the disturbance in glucose metabolism and reverse the dysbiosis of gut microbiota in diabetic mice. Carbohydr Polym 190: 77-86, 2018.
37. Xu Q, Liu M, Liu Q, Wang W, Du Y and Yin H: The inhibition of LPS-induced inflammation in RAW264.7 macrophages via the PI3K/Akt pathway by highly N-acetylated chitooligosaccharide. Carbohydr Polym 174: 1138-1143, 2017.
38. Livak KJ and Schmittgen TD: Analysis of relative gene expression data using real-time quantitative PCR and the 2(-Delta Delta C(T)) method. Methods 25: 402-408, 2001.
39. Wang H, Ge W, Jiang W, Li D and Ju X: SRPK1-siRNA suppresses K562 cell growth and induces apoptosis via the PARP-caspase3 pathway. Mol Med Rep 17: 2070-2076, 2018.
40. Smith AJO, Ball SS, Bowater RP and Wormstone IM: PARP-1 inhibition influences the oxidative stress response of the human lens. Redox Biol 8: 354-362, 2016.
41. Singh R, Letai A and Sarosiek K: Regulation of apoptosis in health and disease: The balancing act of BCL-2 family proteins. Nat Rev Mol Cell Biol 20: 175-193, 2019.
42. Peña-Blanco A and García-Sáez AJ: Bax, Bak and beyond-mitochondrial performance in apoptosis. FEBS J 285: 416-431, 2018.
43. Lan R, Chang Q, An L and Zhao Z: Dietary supplementation with chitosan oligosaccharides alleviates oxidative stress in rats challenged with hydrogen peroxide. Animals (Basel) 10: 55, 2019.
44. Marmouzi I, Ezzat SM, Salama MM, Merghany RM, Attar AM, El-Desoky AM and Mohamed SO: Recent updates in pharmacological properties of chitooligosaccharides. Biomed Res Int 2019: 4568039, 2019.
45. Liu W, Liu Y, Li H and Rodgers GP: Olfactomedin 4 contributes to hydrogen peroxide-induced NADPH oxidase activation and apoptosis in mouse neutrophils. Am J Physiol Cell Physiol 315: C494-C501, 2018.
46. Zhang Y, Ahmad KA, Khan FU, Yan S, Ihsan AU and Ding Q: Chitosan oligosaccharides prevent doxorubicin-induced oxidative stress and cardiac apoptosis through activating p38 and JNK MAPK mediated Nrf2/ARE pathway. Chem Biol Interact 305: 54-65, 2019.
47. Jia P, Yu L, Tao C, Dai G, Zhang Z and Liu S: Chitosan oligosaccharides protect nucleus pulposus cells from hydrogen peroxide-induced apoptosis in a rat experimental model. Biomed Pharmacother 93: 807-815, 2017.
48. Zhu L, Li R, Jiao S, Wei J, Yan Y, Wang ZA, Li J and Du Y: Blood-brain barrier permeable chitosan oligosaccharides interfere with β-amyloid aggregation and alleviate β-amyloid protein mediated neurotoxicity and neuroinflammation in a dose- and degree of polymerization-dependent manner. Mar Drugs 18: 488, 2020.
49. Abate M, Festa A, Falco M, Lombardi A, Luce A, Grimaldi A, Zappavigna S, Sperlongano P, Irace C, Caraglia M and Misso G: Mitochondria as playmakers of apoptosis, autophagy and senescence. Semin Cell Dev Biol 98: 139-153, 2020.
50. Bock FJ and Tait SWG: Mitochondria as multifaceted regulators of cell death. Nat Rev Mol Cell Biol 21: 85-100, 2020.
51. Zheng C, Liu T, Liu H and Wang J: Role of BCL-2 family proteins in apoptosis and its regulation by nutrients. Curr Protein Pept Sci 21: 799-806, 2020.
52. Henning RJ, Bourgeois M and Harbison RD: Poly(ADP-ribose) polymerase (PARP) and PARP inhibitors: Mechanisms of action and role in cardiovascular disorders. Cardiovasc Toxicol 18: 493-506, 2018.
53. Huang H, Ouyang Q, Mei K, Liu T, Sun Q, Liu W and Liu R: Acetylation of SCFD1 regulates SNARE complex formation and autophagosome-lysosome fusion. Autophagy 19: 189-203, 2023.
54. Dong X, Shu L, Zhang J, Yang X, Cheng X, Zhao X, Qu W, Zhu Q, Shou Y, Peng G, *et al*: Ogt-mediated O-GlcNAcylation inhibits astrocytes activation through modulating NF-κB signaling pathway. J Neuroinflammation 20: 146, 2023.